Letter

Momentum imaging of electrons and recoil ions from anion–neutral interactions in a cryogenic ion storage ring

F. Herrmann,[1] W. Zhang,[1] M. Schulz,[1,2] D. V. Chicharro,[1] A. Dorn,[1] M. Grieser,[1] F. Grussie,[1] H. Kreckel,[1] O. Novotny,[1] F. Trost,[1] A. Wolf,[1] T. Pfeifer,[1] C. D. Schröter,[1] and R. Moshammer[1]

[1]*Max-Planck-Institute for Nuclear Physics, Saupfercheckweg 1, D-69117 Heidelberg, Germany*

[2]*Missouri University of Science & Technology, Physics Department and Laboratory for Atomic, Molecular, and Optical Research, Rolla, Missouri 65409, USA*

(Received 13 December 2024; revised 29 January 2025; accepted 11 March 2025; published 25 March 2025)

We have momentum-analyzed electrons and recoil ions in triple coincidence with projectiles neutralized in 300-keV $Si^- + Ar$ collisions. The experiment was performed at a cryogenic ion storage ring with an in-ring reaction microscope. Differential momentum distributions for detachment with simultaneous target ionization were obtained. At more than 15% of the detachment-only rate the ionization rate is surprisingly large. A correlated two-electron channel is found to be dominant. This is also unexpected because the projectile energy is well below the threshold for the correlated process.

DOI: 10.1103/PhysRevResearch.7.L012082

The dynamics of systems of n electrically charged particles is a complex problem for $n \geqslant 3$ [known as the few-body problem (FBP)] because the Schrödinger equation is not analytically solvable for more than two mutually interacting particles (e.g., [1,2]). For collisions of nonstructured projectiles (electrons or bare ions) with simple atoms, a rich literature exists on studies of the FBP by measuring or calculating multiple differential cross sections of various reaction channels (e.g., [3,4] and references therein). In contrast, for structured projectiles, especially for negatively charged ions, the literature is not as comprehensive.

When structured ions and/or atoms collide with each other a multitude of interparticle interactions are present, which can cause transitions of electrons within the collision system. The core of the projectile may interact with an electron bound to the target, the core of the target with an electron bound to the projectile, and electrons bound to the respective other collision partner can interact with each other. This can result in processes, among others, in which electrons are ejected from each of the two collision partners. In the case of negatively charged projectiles, we refer to this process as detachment with simultaneous target ionization (DI). Detachment without target ionization (DE) has been studied extensively for many years (e.g., [5–21]). The literature is equally rich on pure target ionization (without detachment) by charged particle impact and many review articles are available (e.g., [4,22,23]). However, the literature on studies of DI is not nearly as comprehensive (e.g., [24–27]). As a result, our understanding of the underlying reaction dynamics, i.e., the temporal evolution of the system under the influence of the interparticle forces causing the transition, is still rather incomplete.

Target ionization by positive ion impact is one of the most basic processes occurring in atomic collisions. In the case of bare ions, the primary interaction causing the transition is necessarily the one between the projectile core (i.e., the nucleus) and the active target electron. But even for structured projectiles this interaction tends to dominate the ionization process because the effective nuclear charge is generally larger than the charge of the electrons. In contrast, in the case of DI by anion impact it is not immediately clear that the projectile core–target electron interaction plays a similarly prominent role. This interaction alone would only remove an electron from the target, but not from the projectile. The ejection of a projectile electron, completing DI, would require its interaction with the target core as an additional reaction step. This represents a higher-order process, which tends to be much weaker than first-order processes. Furthermore, the core of the anion, seen from a large distance, is neutral and thus should be relatively inefficient in ionizing the target. A possibly more likely scenario may be that both electrons are removed from the respective collision partner by a single mutual interaction with each other (electron-electron interaction, V_{ee}). We refer to this as a correlated first-order two-electron process. At large projectile energies and for other processes involving the simultaneous transition of a projectile electron and a target electron it is well known that such first-order processes are often important if not dominant (e.g., [28,29]).

At small projectile energies, however, the V_{ee} interaction is expected to be much less important. The electron affinity of an anion tends to be rather small (1.4 eV for Si^- [30]). One can then model the active projectile electron as quasi-free. For a truly free electron there would be a threshold energy K_{min} (15.76 eV for Ar) below which the process is kinematically prohibited. For a (weakly) bound electron, it is its momentum distribution in the initial bound state (the Compton profile)

Published by the American Physical Society under the terms of the Creative Commons Attribution 4.0 International license. Further distribution of this work must maintain attribution to the author(s) and the published article's title, journal citation, and DOI. Open access publication funded by Max Planck Society.

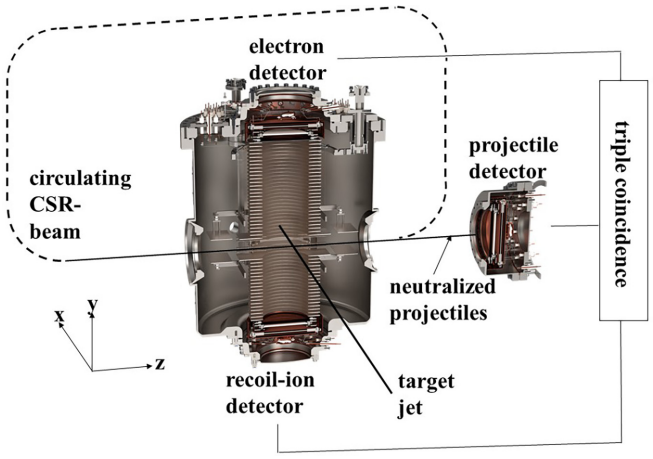


FIG. 1. Schematic of the experimental setup.

that can make the first-order process possible even below this threshold if the vector sum of the projectile velocity and the electron momentum in the Compton profile becomes sufficiently large. Nevertheless, the probability for the electron to have the "right" momentum in the initial state is small (approximately 10–15% for our collision system [14]) and the cross section should rapidly approach zero as the projectile energy drops below the threshold for a truly free electron.

Because of the small DI cross section initially expected at projectile energies below the threshold it was considered critical to use large projectile beam intensities and ultrahigh vacuum to achieve very small background-signal levels. The Max-Planck Institute for Nuclear Physics in Heidelberg (MPI-K) operates a facility satisfying these requirements, the cryogenic storage ring (CSR) [31]. On the detection side, an established multiparticle coincidence measurement tool in atomic physics is known as a reaction microscope (ReMi) [32]. It enables measuring the momenta of the recoiling target ions and electrons produced in a collision or by photoabsorption with high resolution and with 4π detector solid angles. The combination of the CSR and a ReMi promises detailed insight into the reaction dynamics of few-body processes in atomic collisions. Recently, we presented results using this combination for double-coincidence detection of electrons and neutralized projectiles, studying DE from slow anions in collisions with neutral atoms and molecules [21].

Here, we report triple-coincident multiple differential electron momentum distributions for DI at a projectile energy well below the truly free-electron threshold for the correlated first-order process. Nevertheless, this first-order mechanism appears to be dominant, while no signatures of uncorrelated processes are found. The surprisingly large DI reaction rate (relative to DE) is currently not understood. Apart from serving as a proof-of-principle experiment for the CSR-ReMi combination, we anticipate that the data will trigger theoretical work on this topic and thereby provide insight into the reaction dynamics of correlated two-electron collision processes.

A schematic sketch of the experimental setup is shown in Fig. 1. Si^- ions were produced with a sputter source and stored at an energy of 300 keV for 30 s after each injection. This energy corresponds to a projectile speed of 0.65 a.u., while the threshold for the correlated first-order DI process corresponds to a free-electron speed of larger than 1 a.u. The base vacuum in the storage ring was better than 10^{-12} mbar so that data could be taken essentially free of background from the residual gas. The projectiles neutralized in the collision were separated from the stored beam by electrostatic deflectors located downstream from the target region. They were then detected with a two-dimensional position-sensitive microchannel plate (MCP) detector with an active area of 12 cm in diameter and equipped with a delay-line anode.

The projectile beam was crossed with a very cold ($T < 1$ K) beam of neutral Ar atoms from a supersonic jet. The electrons and the recoiling target ions from the intersection region were detected and momentum-analyzed by a ReMi apparatus described in [21]. Both particles were extracted transversely relative to the projectile beam (due to their opposite charge in opposite directions) by a weak electric field of about 2 V/cm. This electric field was superimposed by a magnetic field of 5 G, which forced the electrons into cyclotron motion. For momenta of <1.5 a.u. perpendicular to the extraction field the cyclotron radius was small enough to confine the electrons to the detector. Further details of the ReMi apparatus will be reported in a forthcoming paper.

From the position information of the ReMi detectors we obtained the two momentum components of the electrons and recoil ions in the plane of the detectors, i.e., the x and z components. The momentum components in the direction of the extraction field, the y components, were calculated from the time-of-flight (TOF) from the collision region to the respective detectors, which, in turn, is contained in the coincidence time. All detectors are operated in multihit mode. This means that the electrons ejected from the projectile and the target were recorded simultaneously. However, if both electrons hit the detector at the same position and/or time, the signals they produce in the detector cannot be separated from each other. The multihit deadtime, i.e., the minimum time separation between two electrons required to resolve the two signals, was about 15 ns.

In Fig. 2 we present the neutralized projectile–recoil-ion coincidence time spectrum, which reflects the TOF of the recoil ions, which in turn, depends on their charge-to-mass ratio. Two pronounced and well separated peaks are clearly visible: the larger peak, at late TOF, is due to $^{40}Ar^+$ ions and thus represents DI. The smaller peak, at earlier TOF, reflects $^{40}Ar^{2+}$ ions and thus can be associated with detachment with simultaneous double target ionization (DDI). The very small peak at 25.5 μs is due to the ^{36}Ar isotope. In the case of $^{40}Ar^+$ the ratio between the peak height and the random background is about 40:1. Therefore, DI is easily observable with our experimental setup at a surprisingly large rate which amounts to 8% of that observed for DE. The DE rate was obtained from the neutral projectile–electron coincidence time spectrum with the additional condition that no valid recoil ion was detected. This anticondition reduces the contributions from DI to the double coincidences, but it does not completely remove it due to the limited detection efficiency. However, since the DI cross section is much smaller than the DE cross section the DE rate is not significantly affected. Even DDI is quite prominent in the time spectrum with a rate which is about 4% of the one for DI. The DI to DE cross-section ratio is to a good

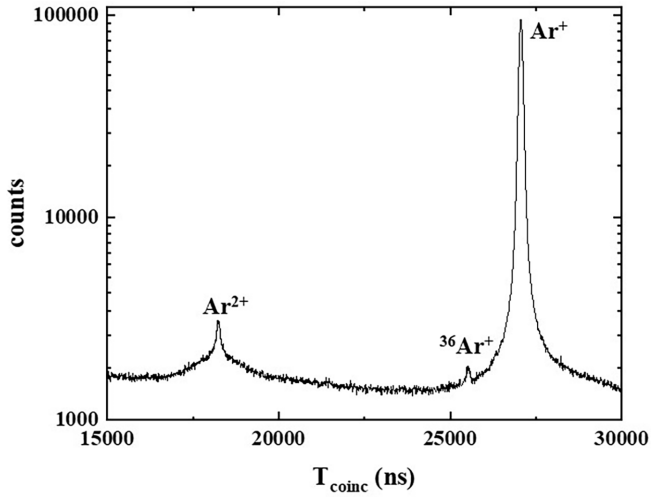


FIG. 2. Time spectrum of the coincidences between neutralized projectiles and recoil ions with contributions from DI and DDI as discussed in the text.

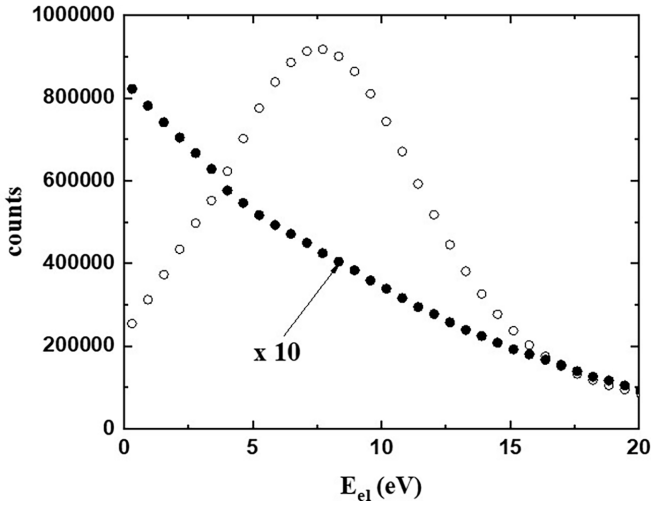


FIG. 4. Energy spectra of electrons ejected in 300-keV $Si^- + Ar$ collisions, showing the first detected electron in coincidence with a neutralized projectile. Open symbols: events where no recoil ion was detected (dominated by DE); closed symbols: events where an Ar^+ recoil ion was detected (dominated by DI).

approximation obtained from the corresponding event rates N by

$$\sigma_{DI}/\sigma_{DE} = (N_{DI}/N_{DE})/[\varepsilon_{rec}2(1-\varepsilon_e)], \quad (1)$$

where ε_{rec} and ε_e are the recoil-ion and electron detection efficiencies. These efficiencies do not differ significantly from each other [33]. For $\varepsilon = \varepsilon_{rec} \approx \varepsilon_e$ the factor $f = 1/[\varepsilon_{rec}2(1-\varepsilon_e)]$ in Eq. (1) only varies between 2 and 3.1 in the range $\varepsilon = 0.2$–0.8 (see Fig. 3). For the efficiencies of the detectors in our setup ($\varepsilon = 0.35$), $f = 2.2$, which yields a lower limit for σ_{DI}/σ_{DE} of 18%.

For two reasons the DI rate was expected to be smaller than the DE rate by a large factor. First, DI involves the transition of two active electrons as opposed to only one in DE. Furthermore, the active target electron, only ejected in DI, has a much larger binding energy than the active electron on the projectile. Therefore, the additional ejection from the target by itself is already expected to reduce the DI rate by a large factor compared to DE. Second, the DI rate is further reduced by the fact that only a small fraction of the Compton profile can contribute to the correlated first-order DI process. Within the quasifree electron model an upper limit for the cross-section ratio between the correlated first-order DI channel and DE can be estimated as follows: The total single detachment cross section was measured for the same collision system and energy to be about 1.1×10^{-15} cm^2 [9]. The target ionization cross section by free electron impact is zero at threshold and then rises with energy until reaching a maximum at about 100 eV [34]. At 300 keV only 10–15% of the projectile electrons have a sufficiently large momentum in the Compton profile [14] to bring their total kinetic energy above the threshold. For these electrons the average kinetic energy is about 20 eV. At this energy the measured ionization cross section by free-electron impact is 5×10^{-17} cm^2 [34]. However, this value represents an overestimation because right above threshold the cross section increases more steeply than above 20 eV. Therefore, the cross section for impact by a single quasifree electron is smaller than 7.5×10^{-18} cm^2. This value needs to be multiplied by a factor of 5 because each Si^- ion is a source of five quasifree electrons. We thus estimate that the cross section for the correlated target ionization process should be $< 4 \times 10^{-17}$ cm^2, i.e., less than 3.5% of the detachment cross section. Therefore, the expected correlated DI process cross section is at least a factor of 5 smaller than the measured value. In the following, we will investigate to what extent the difference to the measured ratio between the DI and detachment cross sections can be explained by the uncorrelated higher-order DI mechanism.

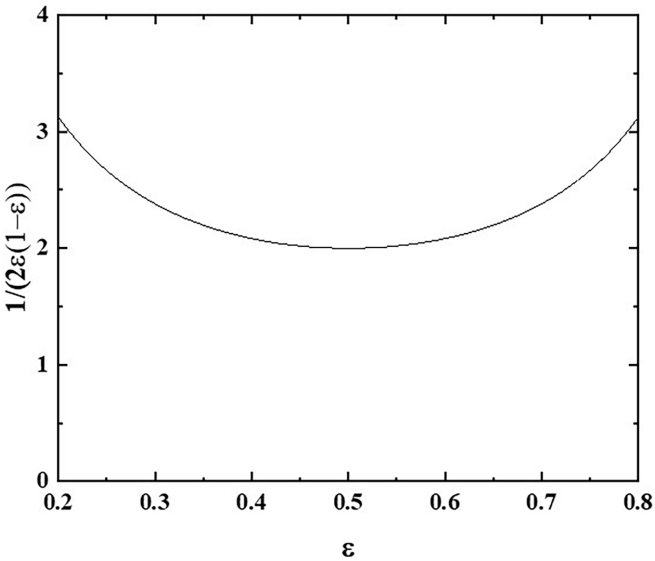


FIG. 3. Correction factor for overall efficiency $1/[\varepsilon_{rec}2(1-\varepsilon_e)]$ in Eq. (1) as a function of ε assuming that $\varepsilon_{rec} = \varepsilon_e = \varepsilon$.

In Fig. 4 we show energy spectra of the electrons ejected in the collision for two different conditions. The data represented by the open symbols were generated under the conditions that no recoil ion and only one electron was detected. Therefore,

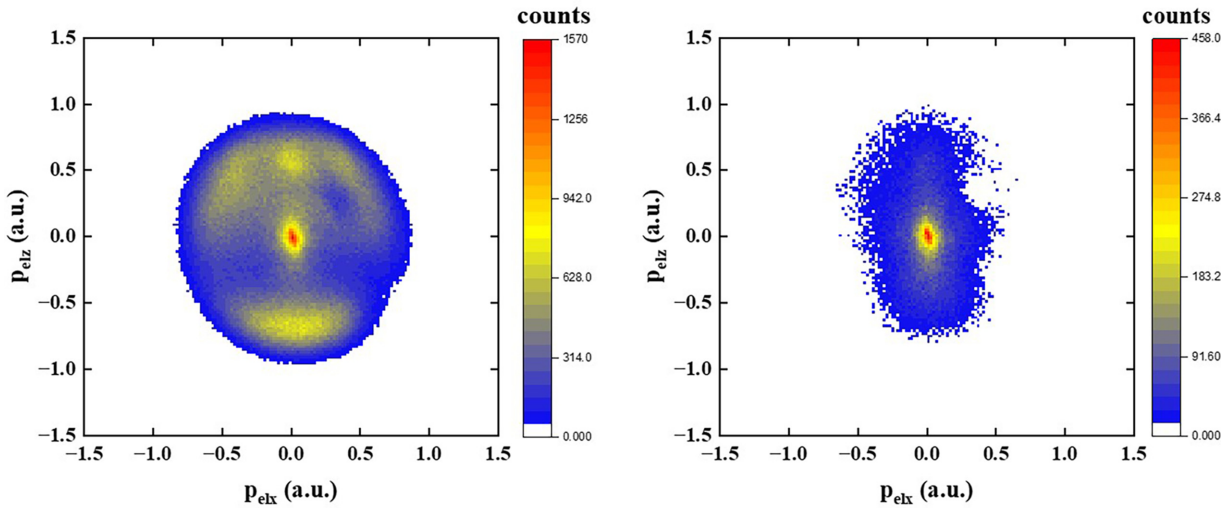


FIG. 5. Two-dimensional momentum spectra of the ejected electrons as a function of the x and z components of the momentum for predominantly DE (left panel) and predominantly DI (right panel) using the same coincidence conditions as applied to the energy spectra of Fig. 4. Additionally, a condition was set on $p_{ely} = 0 \pm 0.05$ a.u. The vertical axis represents the momentum component in the projectile beam direction and the horizontal axis one of the transverse components.

this spectrum represents electrons ejected from DE while DI is strongly suppressed. Indeed, the shape of this energy distribution is consistent with what is expected for DE: in the projectile frame the electrons are most likely ejected with very small speed. Therefore, in the laboratory frame we would expect a maximum near $E_{el} = \frac{1}{2}v_p^2$ a.u. $= 6$ eV. In the measured spectrum, we observe a maximum at 7.5 eV. However, with the same apparatus for 300 keV $Si^- + He$ collisions, we find a maximum at 5 eV, i.e., below the expected position, which makes it unlikely that the deviations are due to inaccuracies in the calibration. The data plotted as closed symbols in Fig. 4 were generated under the condition that a singly charged recoil ion and at least one electron were detected and thus represent DI. To avoid artefacts caused by the multihit deadtime only the first electron hitting the detector was sorted into the histogram, which could arise from either the projectile or the target.

In the uncorrelated higher-order DI process described in the introduction, each electron is ejected by an interaction with the core of the respective other collision partner. Since these two interactions are independent of each other, the shape of the energy spectrum for each electron should be approximately the same as for detachment or target ionization alone. The energy distribution for pure target ionization usually maximizes near 0 eV (e.g., [13]). Therefore for the uncorrelated process we would expect two maxima in the energy spectrum, one at 0 eV and the second at $\frac{1}{2}v_p^2$. For the correlated first-order process without the Compton profile the initial kinetic energy of the projectile electrons would be well below the threshold for target ionization. Hence, this process with high probability forces the projectile electron to give up most of its kinetic energy in the laboratory frame. For the contribution from the correlated channel we would thus expect a single peak around 0 eV in the energy spectrum. In the measured spectrum (Fig. 4) we observe a pronounced maximum at 0 eV and no structure at any other energy. This suggests that the correlated process significantly contributes to DI. On the other hand, the spectrum extends to relatively large energies, e.g., at 15 eV the intensity is still about 10% compared to 0 eV. A maximum at $\frac{1}{2}v_p^2$ could be masked by the strong peak at 0 eV. Therefore, from the energy spectrum alone it is not clear how important the uncorrelated process is.

More detailed information about the reaction dynamics is contained in the two-dimensional momentum spectra of the ejected electrons. These are shown in Fig. 5 as a function of the x and z components of the momenta, with a condition that the y component is 0 ± 0.05 a.u., for pure detachment (left panel) and for DI (right panel). The z direction coincides with the initial projectile beam direction. The minima at about $p_{elx} = p_{elz} = 0.3$ a.u. are due to detector imperfections. It should be noted that these spectra are given by $d^3\sigma/\mathbf{dp^3}$ while the momentum distribution we reported for detachment in [21] was represented as $d^3\sigma/dEd\Omega^2$. Since $d^3\sigma/dEd\Omega^2 = pd^3\sigma/\mathbf{dp^3}$ the strong maximum seen at $p_{elx} = p_{elz} = 0$ (for both DE and DI) was not visible in the momentum distributions presented in [21].

In the case of DE (left panel of Fig. 5) apart from the maximum at $p_{elx} = p_{elz} = 0$ a pronounced ring structure is observed, with a radius equal to the projectile speed. Furthermore, a substructure is visible within the ring, as we have discussed in some detail in [21]. For DI the same structures should be found in the electron momentum spectrum (right panel of Fig. 5) if uncorrelated higher-order channels would significantly contribute. Instead, the momentum distribution for DI exhibits only a single remarkably sharp peak with <0.1 a.u. full width at half maximum around $p_{elx} = p_{elz} = 0$. Not even a trace of a ringlike shape with a radius of the projectile speed can be identified. While the energy spectrum leaves the possibility that the uncorrelated process is contained in the high-energy wing, the absence of a ringlike structure in the momentum distribution strongly indicates that this process does not play a significant role. It can thus not explain the unexpectedly large rate which we observe for DI relative to detachment.

In summary, we have performed a triple coincidence measurement employing a ReMi spectrometer at the cryogenic ion storage ring in Heidelberg. We measured multiple differential momentum distributions of electrons ejected in detachment with simultaneous target ionization DI from collisions of slow anions with neutral Ar atoms. Unexpectedly large cross section ratios relative to simple detachment were observed, namely >18% for DI and >0.35% for detachment accompanied by double target ionization (DDI). Furthermore, the electron momentum distributions do not contain any signature of uncorrelated higher-order reaction channels. Rather, they are dominated by a correlated first-order mechanism in which both electrons are ejected through a single interaction with each other. The importance of this channel is also surprising, because approximating the projectile electron as unbound, the kinetic energy of the projectile electron is well below the threshold for target ionization.

For more systematic future studies of DI and DDI we envision to focus on $H^- + He$ collisions, which should be more amenable to theoretical calculations. Furthermore, we plan to measure cross sections for a broad range of projectile energies, starting well below the threshold for the correlated process up to well above the threshold. The relative importance of the correlated and uncorrelated processes should change significantly between the two ends of this range, which, in turn, should be reflected in sensitive changes to the shape of the electron momentum distributions.

M.S. is grateful for the hospitality of the Max-Planck Institute for Nuclear Physics and for a research scholarship from the Max-Planck Society.

The data that support the findings of this article are not publicly available. The data are available from the authors upon reasonable request.

[1] T. N. Rescigno, M. Baertschy, W. A. Isaacs, and C. W. McCurdy, Collisional breakup in a quantum system of three charged particles, Science **286**, 2474 (1999).

[2] M. Schulz, R. Moshammer, D. Fischer, H. Kollmus, D. H. Madison, S. Jones, and J. Ullrich, Three-dimensional imaging of atomic four-body processes, Nature (London) **422**, 48 (2003).

[3] H. Ehrhardt, K. Jung, G. Knoth, and P. Schlemmer, Z. Phys. D **1**, 3 (1986).

[4] M. Schulz, in *Ion-Atom Collisions. The Few-Body Problem in Dynamic Systems*, edited by M. Schulz (deGruyter, Berlin, 2019), pp. 11–34.

[5] A. K. Edwards, in *The Physics of Electronic and Atomic Collisions*, edited by J. S. Risley and R. Geballe (University of Washington, Seattle, 1975), pp. 790–799.

[6] V. A. Esaulov, Electron detachment from atomic negative ions, Ann. Phys. Paris **11**, 493 (1986).

[7] D. J. Pegg, Structure and dynamics of negative ions, Rep. Prog. Phys. **67**, 857 (2004).

[8] F. Zappa, G. Jalbert, L. F. S. Coelho, A. B. Rocha, S. D. Magalhães, and N. V. de Castro Faria, Absolute electron detachment cross sections of atomic anions of the second and third periods incident on noble gases, Phys. Rev. A **69**, 012703 (2004).

[9] H. Luna, F. Zappa, M. H. P. Martins, S. D. Magalhães, G. Jalbert, L. F. S. Coelho, and N. V. de Castro Faria, Comparative study of the collisional electron detachment of C^-, Si^-, and Ge^- by light noble gases, Phys. Rev. A **63**, 052716 (2001).

[10] B. Hird and F. Rahman, Charge neutralization of F^- ions in thin rare-gas targets, Phys. Rev. A **26**, 3108 (1982).

[11] N. Andersen, T. Andersen, L. Jepsen, and J. Macek, Electron detachment processes in keV H^-, Li^-, Na^-, K^--rare-gas collisions, J. Phys. B **17**, 2281 (1984).

[12] J. S. Risley, Comparison of H^- and D^- detachment cross sections, Phys. Rev. A **10**, 731 (1974).

[13] X. M. Zhang, S. M. Wu, G. W. Li, F. Q. Lu, J. Y. Tang, and F. J. Yang, Measurements of single-electron detachment cross-sections for Cu^- and Ag^- in collision with He and N^2, Europhys. Lett. **56**, 797 (2001).

[14] G. Jalbert, W. Wolff, S. D. Magalhaes, and N. V. de Castro Faria, Electron detachment of negative ions: The influence of the outermost electron and its neutral core atom in collision with He, Ne, and Ar, Phys. Rev. A **77**, 012722 (2008).

[15] G. M. Sigaud, Free-collision model calculations for the electron detachment of anions by noble gases, J. Phys. B **41**, 015205 (2007).

[16] T. Andersen, Atomic negative ions: Structure, dynamics and collisions, Phys. Rep. **394**, 157 (2004).

[17] J. S. Risley, in *Proceedings of the 11th International Conference on the Physics of Electronic and Atomic Collisions*, *Kyoto* 1979, edited by N. Oda and K. Takayanagi (North-Holland, Amsterdam, 1980), p. 619.

[18] Y. N. Demkov and V. N. Ostrovsky, *Zero-Range Potentials and their Applications in Atomic Physics* (Plenum, New York, 1988).

[19] J. P. Gauyacq, Theoretical study of the detachment process in the zero-range potential approximation. H^- − He collisions, J. Phys. B **13**, 4417 (1980).

[20] J. P. Connerade and V. N. Ostrovsky, Electron detachment in collisions of negative ions with non-metallic clusters, J. Phys. B **35**, L475 (2002).

[21] M. Schulz, F. Herrmann, W. Zhang, D. V. Chicharro, A. Dorn, M. Grieser, F. Grussie, H. Kreckel, O. Novotny, F. Trost, A. Wolf, T. Pfeifer, C. D. Schröter, and R. Moshammer, Multiple differential electron spectra from detachment in collisions of 30−300-keV anions with atoms and molecules, Phys. Rev. A **110**, 022818 (2024).

[22] M. E. Rudd, Y. K. Kim, D. H. Madison, and T. J. Gay, Electron production in proton collisions with atoms and molecules: energy distributions, Rev. Mod. Phys. **64**, 441 (1992).

[23] N. Stolterfoht, R. A. Rivarola, and R. D. Dubois, *Electron Emission in Heavy Ion-Atom Collisions* (Springer, Berlin, 1997).

[24] L. H. Andersen, L. B. Nielsen, and J. Sörensen, Single and double ionisation of He and Ar by far H^0 and H^- projectiles, J. Phys. B **21**, 1587 (1988).

[25] F. Zappa, A. L. F. de Barros, L. F. S. Coelho, G. Jalbert, S. D. Magalhaes, and N. V. de Castro Faria, Ionization of helium by impact of negative B, O, and F ions, Phys. Rev. A **70**, 034701 (2004).

[26] Z. Zhao, J. Li, and X. Zhang, Experimental study of ionization of Ar by impact of anions, Nucl. Instrum. Methods Phys. Res. B **283**, 35 (2012).

[27] M. Schulz, T. Ferger, D. Fischer, R. Moshammer, and J. Ullrich, Multiple scattering mechanisms in simultaneous projectile-electron and target-electron ejection in $H^- + He$ collisions, Phys. Rev. A **74**, 042705 (2006).

[28] J. A. Tanis, E. M. Bernstein, W. G. Graham, M. P. Stockli, M. Clark, R. H. McFarland, T. J. Morgan, K. H. Berkner, A. S. Schlachter, and J. W. Stearns, Resonant electron transfer and excitation in two-, three-, and four- electron $_{20}Ca^{q+}$ and $_{23}V^{q+}$ ions colliding with helium, Phys. Rev. Lett. **53**, 2551 (1984).

[29] E. C. Montenegro, W. E. Meyerhof, and J. H. McGuire, Role of two-center electron-electron interaction in projectile electron excitation and loss, Adv. At. Mol. Opt. Phys. **34**, 249 (1994).

[30] M. Scheer, R. C. Bilodeau, C. A. Brodie, and H. K. Haugen, Systematic study of the stable states of C^-, Si^-, Ge^-, and Sn^- via infrared laser spectroscopy, Phys. Rev. A **58**, 2844 (1998).

[31] R. von Hahn *et al.*, The cryogenic storage ring CSR, Rev. Sci. Instrum. **87**, 063115 (2016).

[32] J. Ullrich, R. Moshammer, A. Dorn, R. Dörner, L. Ph. H. Schmidt, and H. Schmidt-Böcking, Recoil-ion and electron momentum spectroscopy: Reaction-microscopes, Rep. Prog. Phys. **66**, 1463 (2003).

[33] J. L. Wiza, Microchannel plate detectors, Nucl. Instrum. Methods **162**, 587 (1979).

[34] H. Tawara and T. Kato, Total and partial ionization cross sections of atoms and ions by electron impact, At. Data Nucl. Data Tables **36**, 167 (1987).